Stabilization and Manipulation of Electronically Phase-Separated Ground States in Defective Indium Atom Wires on Silicon

Hui Zhang,[1] Fangfei Ming,[2] Hyun-Jung Kim,[3] Hongbin Zhu,[1] Qiang Zhang,[1] Hanno H. Weitering,[4,5] Xudong Xiao,[2,6] Changgan Zeng,[1,7,8,*] Jun-Hyung Cho,[3,†] and Zhenyu Zhang[7,8]

[1]*Hefei National Laboratory for Physical Sciences at the Microscale (HFNL) and Department of Physics, University of Science and Technology of China, Hefei, Anhui 230026, China*
[2]*Department of Physics, The Chinese University of Hong Kong, Shatin, New Territory, Hong Kong, China*
[3]*Department of Physics, Hanyang University, 17 Haengdang-Dong, SeongDong-Ku, Seoul 133-791, Korea*
[4]*Department of Physics and Astronomy, The University of Tennessee, Knoxville, Tennessee 37996, USA*
[5]*Materials Science and Technology Division, Oak Ridge National Laboratory, Oak Ridge, Tennessee 37831, USA*
[6]*Shenzhen Institute of Advanced Technology, Chinese Academy of Science, Shenzhen 518055, China*
[7]*International Center for Quantum Design of Functional Materials (ICQD), HFNL, University of Science and Technology of China, Hefei, Anhui 230026, China*
[8]*Synergetic Innovation Center of Quantum Information and Quantum Physics, University of Science and Technology of China, Hefei, Anhui 230026, China*

(Received 8 June 2014; revised manuscript received 31 August 2014; published 6 November 2014)

Exploration and manipulation of electronic states in low-dimensional systems are of great importance in the fundamental and practical aspects of nanomaterial and nanotechnology. Here, we demonstrate that the incorporation of vacancy defects into monatomic indium wires on *n*-type Si(111) can stabilize electronically phase-separated ground states where the insulating 8×2 and metallic 4×1 phases coexist. Furthermore, the areal ratio of the two phases in the phase-separated states can be tuned reversibly by electric field or charge doping, and such tunabilities can be quantitatively captured by first principles-based modeling and simulations. The present results extend the realm of electronic phase separation from strongly correlated *d*-electron materials typically in bulk form to weakly interacting *sp*-electron systems in reduced dimensionality.

DOI: 10.1103/PhysRevLett.113.196802 PACS numbers: 73.20.At, 68.35.Rh, 68.37.Ef

Metal-atom adsorption on semiconductor surfaces often results in the formation of quasi-one or two-dimensional electron systems that are susceptible to charge density wave instabilities [1], Luttinger liquid correlations [2], and magnetic [3,4] or superconducting [5,6] ordering at low temperatures. Each of these established ground states in such electronically simple systems is homogeneous in nature [7]. In contrast, in strongly correlated electron systems such as doped manganite compounds, different electronic states are often found to be in close proximity thermodynamically, and electronically phase-separated (PS) ground states can be stabilized by quenched disorder [8] or strain [9].

Previous examples of electronic phase separation have so far been limited to strongly correlated *d*-electron systems involving delicate coupling and competitions between the spin, charge, lattice, and orbital degrees of freedom [10–12]. Thus, it is conceptually intriguing to explore the feasibility of stabilizing electronically PS ground states in simple *sp*-electron systems, where the underlying mechanisms are likely to be more readily revealed and manipulated. Meanwhile, it has been demonstrated that the surface structures of adatoms on semiconductors [for example, Si(100) surface [13], α-Pb/Ge(111) [14], Au/Si(553) [15], and α-Sn/Ge(111) [16]] can be manipulated effectively at low temperatures, and such tunabilities have been attributed to electric field [17], charging effect [14,15], or inelastic tunneling processes [16].

In this Letter, we present the first demonstration that by incorporating vacancy defects, electronically PS ground states can be stabilized in In atom wires on *n*-type Si(111), where the electrons move in broad $5sp$ bands. In addition, these PS states encompassing the insulating 8×2 and metallic 4×1 phases can be effectively manipulated to tune the areal ratio of the two phases by changing the tunneling conditions. Such phenomena of phase control can be quantitatively captured by first-principles density functional theory (DFT) calculations.

The indium atom wires on the Si(111) surface undergo a reversible phase transition from a metallic 4×1 high-temperature phase [Fig. 1(a)] to an 8×2 insulating phase at about 130 K [18,19]. Previous temperature-dependent scanning tunneling microscopy (STM) studies mainly focused on the nature of the phase transition [20–29], including order of the transition [20–24] and tunability of the transition temperature [25–27].

The defect density of the In/Si(111) system can be varied over a relatively wide range by changing the In deposition flux as shown in Fig. S1 in the Supplemental Material [30]: lowering the deposition flux increases the density of the surface defects. Here, the defects most

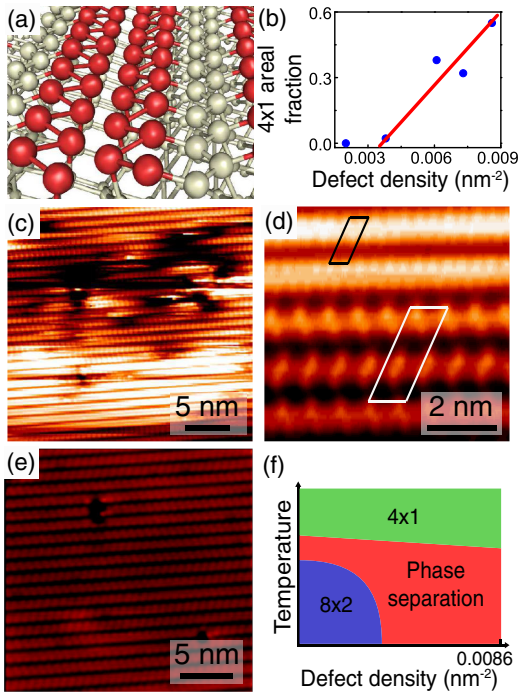

FIG. 1 (color online). (a) Perspective view of the optimized 4×1 structure. (b) Areal fraction of the 4×1 phase at 78 K as a function of the defect density. (c), (d) STM images of a defect-rich sample ($\rho = 0.0073$ nm^{-2}) at 5 K, with $V_s = -1.0$ V, $I_t = 0.5$ nA for (c), and $V_s = -1.0$ V, $I_t = 1.5$ nA for (d). (e) STM image of a defect-poor sample ($\rho = 0.0038$ nm^{-2}) at 5 K, with $V_s = 1.0$ V, $I_t = 0.5$ nA. (f) Schematic phase diagram for the In/Si(111) system. The unit cells for the 8×2 and 4×1 phases are indicated in (d).

likely consist of clusters of adatom vacancies, and the random and quenched nature of the defects are revealed in the STM images. The defect density is defined as the number of defects per square nanometer. A similar flux dependence of the defect concentration has also been reported for Ga on Si(112) [31], implying that the defect formation energy is directly related to the chemical potential of the incoming adatom species.

In the limit of low defect density, the $4 \times 1 \leftrightarrow 8 \times 2$ phase transition near 130 K is quite sharp and 4×1 patches associated with the high-temperature phase are almost absent at 100 K [20–22]. In this regime, the 8×2 structure is the true ground state structure. However, at a defect density of $\rho = 0.0073$ nm^{-2}, the insulating 8×2 and metallic 4×1 phases coexist in roughly equal populations at 78 K, i.e., well below 130 K. This can be seen in the STM images of Fig. S2 [30] where the dark patches are the insulating 8×2 phase and the bright patches are the metallic 4×1 phase. Figure 1(b) shows the areal fraction of the 4×1 phase as a function of the defect density, all measured at 78 K, with the sample bias (V_s) ~ 0.5 V and tunneling current (I_t) smaller than 0.5 nA. Interestingly, the areal fraction of the metallic 4×1 phase increases with the defect density. Evidently, in highly defective samples, both phases can be stabilized to coexist at temperatures below 130 K, which is the phase transition temperature for the nearly defect-free system (Fig. S3 in the Supplemental Material [30]).

Strikingly, the phase separation persists down to 5 K for defect-rich samples (for example, at $\rho = 0.0061$ nm^{-2}, 0.0073 nm^{-2}, and 0.0086 nm^{-2}). Figures 1(c) and 1(d) ($\rho = 0.0073$ nm^{-2}) clearly reveal the coexistence of the 8×2 and 4×1 phases at different magnifications. The areal fraction of the metallic 4×1 phase is $\sim$30% at $V_s = -1.0$ V. The observation of the 4×1 structure at temperatures as low as 5 K also suggests that it is a static phase, rather than the average of dynamically fluctuating phases. The relative areal fractions remain unchanged after cycles of annealing to room temperature and cooling down again. The fact that the metallic 4×1 phase has not been completely converted into the insulating 8×2 phase even at 5 K irrespective of cooling rate, strongly suggests that the PS configuration reflects a true ground state. We can sketch a phase diagram for the In/Si(111) system as a function of the defect density and temperature as shown in Fig. 1(f). At 5 K, the 4×1 phase appears with ρ larger than 0.0061 nm^{-2}, whereas it is absent with ρ smaller than 0.0038 nm^{-2} [Fig. 1(e)], regardless of the bias and tunneling current. Therefore, the critical defect density for the phase transition from the pure 8×2 state to the electronically PS state at 5 K is roughly between 0.0038 and 0.0061 nm^{-2}.

Now, we focus on the defect-stabilized phase-separated state, as well as the phase transition of this state to either of its two constituent states under different driving forces. The first is the temperature-driven transition between the homogeneous 4×1 state and phase-separated state at a fixed defect density; the second is the defect-driven transition between the homogeneous 8×2 state and phase-separated state at a fixed low temperature. Although we cannot reliably determine the precise orders of these two phase transitions, they are unlikely to be first order, as shown theoretically that a sufficiently large amount of disorder can change a sharp first-order transition into a continuous one in low-dimensional systems [32] or strongly correlated manganites [8]. The order parameter for either of these two phase transitions can be uniquely defined by the areal fraction of the 8×2 or 4×1 structure, similar to that adopted in a previous study [21]. Whereas the transition between the 4×1 state and phase-separated state is temperature driven, the defect-driven transition between the 8×2 state and phase-separated state is attributed to be a quantum phase transition, whose existence has been demonstrated down to the lowest accessible temperature of 5 K. The randomly distributed defects impose an inhomogeneous strain field (as discussed later) on the In chains, and trigger the phase transition when the induced nonuniform strain is strong enough. This scenario

is in analogy with a picture in the related fields of strongly correlated manganites, where inhomogeneous strain may also drive similar phase transitions [9,10].

We note that the 8×2 insulating phase is formed via a periodic lattice distortion resulting in the formation of In hexagons [33–35]. Thus, it is expected that the existence of a defect-induced local strain field may change the relative stabilities of the 8×2 and 4×1 phases in the In/Si(111) system. Given the inhomogeneous spatial distributions of both the defects and strain field, the resulting surface is found to be covered by regions of the 8×2 and 4×1 phases, whose ratio can be tuned by the defect density. To confirm this picture quantitatively, we perform hybrid DFT calculations, including van der Waals interactions. Since the 8×2 unit cell contains two 4×2 subunits, we can simply compare the total energy difference $\Delta E_{4\times2-4\times1}$ between the 4×2 hexagon and undistorted 4×1 structure. The strain field can also be conveniently modeled by varying the lattice constant of the Si(111) substrate.

Figure 2 shows $\Delta E_{4\times2-4\times1}$ for four different Si lattice constants (the electric field effect will be discussed later). At zero field, $\Delta E_{4\times2-4\times1}$ decreases with the lattice constant: i.e., $\Delta E_{4\times2-4\times1}$ is -15.35, -12.65, -4.23, and -1.51 meV per 4×1 unit cell at $1.002a_0$, a_0 ($= 5.418$ Å, theoretical equilibrium lattice constant), $0.997a_0$, and $0.990a_0$, respectively. These results indicate that compressive strain tends to stabilize the 4×1 structure relative to the 4×2 structure, and that the 4×1 structure ultimately becomes the ground state structure below the threshold strain of $\sim 0.985a_0$.

To make a closer connection with the experiment, we note that the creation of In vacancies leads to finite wire lengths, which, in turn, reduces the lattice distortions associated with the 8×2 phase near the wire ends. Indeed, our DFT calculations with a single-adatom vacancy model confirm that the zigzag In wires contract upon the introduction of In vacancies (Fig. S4 in the Supplemental Material [30]). Note that a decrease of the Si lattice constant would have a similar effect on the zigzag chain. Thus, it is reasonable that the stabilization of the 4×1 structure with increasing defect concentration is the result of defect-induced strain, an underlying mechanism also proposed to be operative for electronic inhomogeneities in manganites [9]. Although the present simplified vacancy model captures the central physics involved in stabilizing the phase-separated ground states, the detailed vacancy structural model should be further investigated in future studies.

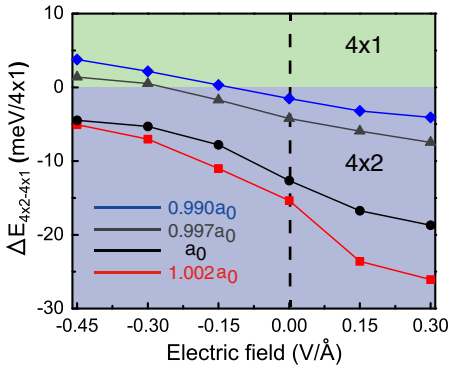

FIG. 2 (color online). Energy difference $\Delta E_{4\times2-4\times1}$ per 4×1 unit cell between the 4×1 and 4×2 structures. The calculated results are for four Si lattice parameters as a function of the external electric field.

In previous studies [20–22], the coexistence of the 4×1 and 8×2 phases was demonstrated in the intermediate temperature range around ~ 120 K, with the 4×1 phase pinned by the adatom vacancy defects. The defects were much lower in total density, and seem to be predominately point defects. In contrast, in the present study, we intentionally created much higher densities of adatom vacancies by tuning the effusion cell temperature, so that, in essence, those high-density defects become vacancy clusters. As a vitally important consequence, we managed to establish the ground-state nature of the electronic phase separation down to 5 K. Moreover, as a further reflection of the delicate competition between the 8×2 and 4×1 phases, next, we show that their areal ratio in the PS states can be tuned reversibly by changing the tunneling conditions.

Figures 3(a) and 3(b) show STM images, recorded at 78 K, with $V_s = -0.4$ V and 0.4 V, respectively, at $\rho = 0.0086$ nm^{-2}. *A*-type (*B*-type) domains at both biases correspond to the 8×2 (4×1) phase. However, *C*-type areas exhibit the 8×2 (4×1) phase at $V_s = 0.4$ V (-0.4 V), indicating that the 8×2 structure transforms into the 4×1 structure and vice versa as the tunneling bias changes its polarity. I–V spectra were also acquired for the *A*-, *B*-, and *C*-type areas, as shown in Fig. 3(c). The typical I–V spectrum for area *A* shows a band gap of about 0.23 V, consistent with previous results [34,36]. For *B*-type areas, the I–V curve reveals metallic behavior. In contrast, for

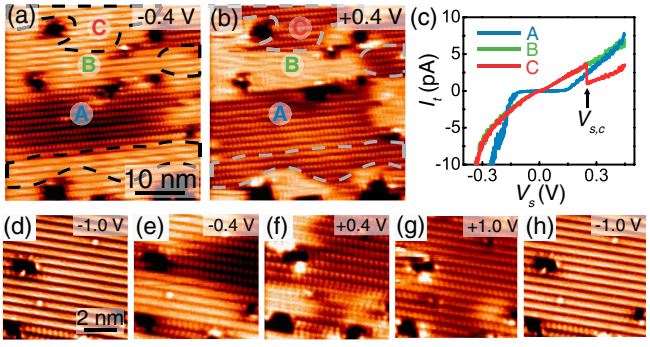

FIG. 3 (color online). Reversible phase transition induced by a local electric field. (a), (b) STM images of the same area at 78 K, with $I_t = 0.03$ nA for both images. *C*-type areas are marked with dashed lines. (c) Typical I–V spectra for the three areas labeled in (a). (d)–(h) Sequential STM images of the same area, with $I_t = 0.05$ nA for (e) and (f), and $I_t = 2.0$ nA for (d), (g), and (h). All the STM images were taken on an *n*-type sample with $\rho = 0.0086$ nm^{-2}.

C-type areas, the tunneling current drops sharply at the critical bias of $V_{s,c} = 0.28$ V, indicating a transition from the metallic 4×1 phase (below 0.28 V) to the insulating 8×2 phase (above 0.28 V). The precise value of the critical bias producing the nanoscale 4×1 to 8×2 tunability fluctuates even at the same location. Such jumps of similar physical origin had also been reported previously [37].

As the bias sweeps from negative to positive, the areal fraction of the 4×1 phase is found to monotonically decrease from 91% at −1.0 V, to being 57% at −0.4 V, 29% at 0.4 V, and 20% at 1.0 V [Figs. 3(d)–3(g)]. The reversibility of such bias control is demonstrated by Figs. 3(d) and 3(h). Such tunable behavior might be induced by an applied electric field [37] or local heating. If the local heating effect were prevailing, it should be more profound in Fig. 3(g) (1.0 V, 2 nA) than in Fig. 3(f) (0.4 V, 0.05 nA), leading to a higher areal fraction of the high-temperature 4×1 phase in Fig. 3(g). On the contrary, the actual experimental results show just the opposite behavior, confirming that the local heating effect should be negligible. Here, we focused on the tunability of the $4 \times 1/8 \times 2$ ratio at the nanoscale within the same defect-stabilized phase-separated state by an applied electric field or charge doping, with the latter discussed later. We also note that, given the largely continuous and nanoscale nature of the tunability demonstrated within the phase-separated state, it is unlikely to expect hysteretic behavior in such systems.

In order to gain a quantitative understanding of the bias-dependent stabilization of the insulating and metallic phases of In/Si(111), we have simulated the electric field effect by superimposing a sawtooth potential along the [111] direction (taken as the $+z$ direction) on top of the effective potential in the Kohn-Sham equation. As shown in Fig. 2, the application of the external electric field along the $+z$ ($-z$) direction decreases (increases) $\Delta E_{4\times2-4\times1}$, enhancing the relative stability of the 4×2 (4×1) phase. This provides a likely explanation for the observed conversion of the insulating 8×2 phase into the metallic 4×1 phase at negative sample bias or, equivalently, negative electric field. Experimentally, a typical sample bias of 0.5 V and a tip-sample distance of 5 Å would give rise to an electrical field of 0.1 V/Å, which is comparable to the theoretically estimated field needed to switch the stability of the two phases under a finite compressive strain. A detailed understanding of the correlation between the phase preference and bias polarity is given in the Supplemental Material [30].

Given the substantially different electronic nature of the two coexisting phases, it is naturally expected that intentional charge doping may serve as another control knob for tuning their relative stability. Such tunability is demonstrated using two different approaches. The first is to take advantage of the different charge transfers between the In atom wires and n- or p-type Si substrate. So far, all observations were made on n-type Si(111) substrates. In sharp contrast, only the pure insulating 8×2 phase is observed for In wires grown on p-type Si(111) substrates (0.017 Ohm · cm) at low temperatures, even for a defect-rich sample ($\rho = 0.0085$ nm^{-2}), as shown in Fig. S6 in the Supplemental Material [30]. The contrasting behaviors on the p- and n-type Si substrates can be attributed to the fact that electron doping helps to stabilize the 4×1 phase [27], while hole doping favors the 8×2 phase. These observations also suggest that the observed PS ground state for defect-rich In wires on n-type substrates is thermodynamically stabilized, instead of kinetically frozen.

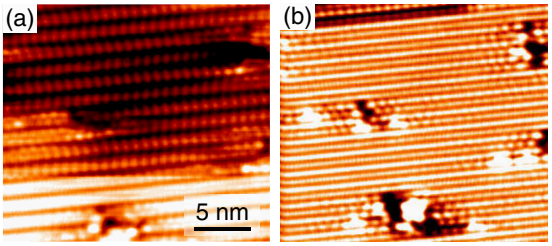

FIG. 4 (color online). Tuning the electronic phase separation by charging effect. (a), (b) STM images of the same area on a sample with $\rho = 0.0061$ nm^{-2} at 5 K, $V_s = -1.0$ V, $I_t = 0.01$ nA for (a); $V_s = 1.0$ V, $I_t = 0.01$ nA for (b).

In the second approach, we restrict ourselves with n-type substrates, but amplify the charging effect at Si surfaces at very low temperatures [14,15,38,39] using different bias potentials. We observe that, at 5 K, positive (negative) V_s favors the 4×1 (8×2) phase (Fig. 4), just opposite to the bias-dependent phase preference at 78 K. This might be explained by the fact that, at such a low temperature, the charge transfer between the In wires and the substrate is substantially suppressed [14,15,38,39], making the tunneling-induced surface charging effect more pronounced. More data and discussion on the proposed competition between the surface charging and the electric field effect are shown in the Supplemental Material [30].

It is noteworthy that the In wires (sp-electron systems) and the strongly correlated manganites (d-electron systems) share similar characteristics. For example, the 8×2 insulating phase in the In wires and the charge ordering phase in manganites are developed by lattice distortions from the metallic phases, respectively. The introduction of extrinsic disorder effects can stabilize electronically PS states in both systems. Moreover, the areal ratio between the metallic phase and the insulating phase can be tuned by external stimulus, e.g., electric or magnetic field or doping.

In summary, we have demonstrated that electronically inhomogeneous states with the coexistence of metallic and insulating phases can be stabilized as true ground states in the In chains on n-type Si(111) substrates after incorporation of vacancy defects. The ratio of the two coexisting phases can be tuned reversibly and effectively by an electric field or charge doping. The present study not only extends the electronic phase separation concept from strongly

correlated *d*-electron systems to *sp*-electron systems on the technologically vital silicon substrates, but also offers new opportunities in manipulating such electronic nanotextures for device applications [40].

H. Z., F. M., and H.-J. K contributed equally to this work. This work was supported in part by the NSFC (Grants No. 11434009, No. 11374279, and No. 11034006), NKBRPC (Grant No. 2014CB921102), CAS (Grant No. XDB01020000), SRFDP (Grant No. 20113402110046), FRFCU (Grants No. WK2340000035 and No. WK2340000011), the NRF (Grant No. 2014M2B2A9032247), and the KISTI supercomputing center through the strategic support program (No. KSC-2013-C3-043). H. H. W. acknowledges support from NSF Grant No. DMR-1005488.

*cgzeng@ustc.edu.cn
†chojh@hanyang.ac.kr

[1] J. M. Carpinelli, H. H. Weitering, E. W. Plummer, and R. Stumpf, Nature (London) **381**, 398 (1996).
[2] C. Blumenstein, J. Schäfer, S. Mietke, S. Meyer, A. Dollinger, M. Lochner, X. Y. Cui, L. Patthey, R. Matzdorf, and R. Claessen, Nat. Phys. **7**, 776 (2011).
[3] S. C. Erwin and F. J. Himpsel, Nat. Commun. **1**, 58 (2010).
[4] G. Li, P. Höpfner, J. Schäfer, C. Blumenstein, S. Meyer, A. Bostwick, E. Rotenberg, R. Claessen, and W. Hanke, Nat. Commun. **4**, 1620 (2013).
[5] S. Qin, J. Kim, Q. Niu, and C. K. Shih, Science **324**, 1314 (2009).
[6] T. Zhang *et al.*, Nat. Phys. **6**, 104 (2010).
[7] P. C. Snijders and H. H. Weitering, Rev. Mod. Phys. **82**, 307 (2010).
[8] J. Burgy, M. Mayr, V. Martin-Mayor, A. Moreo, and E. Dagotto, Phys. Rev. Lett. **87**, 277202 (2001).
[9] K. H. Ahn, T. Lookman, and A. R. Bishop, Nature (London) **428**, 401 (2004).
[10] E. Dagotto, Science **309**, 257 (2005).
[11] V. Kiryukhin, D. Casa, J. P. Hill, B. Keimer, A. Vigliante, Y. Tomioka, and Y. Tokura, Nature (London) **386**, 813 (1997).
[12] M. Rini, R. Tobey, N. Dean, J. Itatani, Y. Tomioka, Y. Tokura, R. W. Schoenlein, and A. Cavalleri, Nature (London) **449**, 72 (2007).
[13] K. Sagisaka, D. Fujita, and G. Kido, Phys. Rev. Lett. **91**, 146103 (2003).
[14] I. Brihuega, O. Custance, M. M. Ugeda, N. Oyabu, S. Morita, and J. M. Gómez-Rodríguez, Phys. Rev. Lett. **95**, 206102 (2005).
[15] S. Polei, P. C. Snijders, S. C. Erwin, F. J. Himpsel, K.-H. Meiwes-Broer, and I. Barke, Phys. Rev. Lett. **111**, 156801 (2013).
[16] S. Colonna, F. Ronci, A. Cricenti, and G. Le Lay, Phys. Rev. Lett. **101**, 186102 (2008).
[17] K. Seino, W. G. Schmidt, and F. Bechstedt, Phys. Rev. Lett. **93**, 036101 (2004).
[18] H. W. Yeom *et al.*, Phys. Rev. Lett. **82**, 4898 (1999).
[19] T. Tanikawa, I. Matsuda, T. Kanagawa, and S. Hasegawa, Phys. Rev. Lett. **93**, 016801 (2004).
[20] S. J. Park, H. W. Yeom, J. R. Ahn, and I. W. Lyo, Phys. Rev. Lett. **95**, 126102 (2005).
[21] J. Guo, G. Lee, and E. W. Plummer, Phys. Rev. Lett. **95**, 046102 (2005).
[22] G. Lee, J. Guo, and E. W. Plummer, Phys. Rev. Lett. **95**, 116103 (2005).
[23] S. Hatta, Y. Ohtsubo, T. Aruga, S. Miyamoto, H. Okuyama, H. Tajiri, and O. Sakata, Phys. Rev. B **84**, 245321 (2011).
[24] F. Klasing, T. Frigge, B. Hafke, B. Krenzer, S. Wall, A. Hanisch-Blicharski, and M. Horn-von Hoegen, Phys. Rev. B **89**, 121107 (2014).
[25] Y. Terada, S. Yoshida, A. Okubo, K. Kanazawa, M. Xu, O. Takeuchi, and H. Shigekawa, Nano Lett. **8**, 3577 (2008).
[26] T. Shibasaki *et al.*, Phys. Rev. B **81**, 035314 (2010).
[27] H. Morikawa, C. C. Hwang, and H. W. Yeom, Phys. Rev. B **81**, 075401 (2010).
[28] S. Wippermann and W. G. Schmidt, Phys. Rev. Lett. **105**, 126102 (2010).
[29] S. Wall, B. Krenzer, S. Wippermann, S. Sanna, F. Klasing, A. Hanisch-Blicharski, M. Kammler, W. Gero Schmidt, and M. Horn-von Hoegen, Phys. Rev. Lett. **109**, 186101 (2012).
[30] See Supplemental Material at http://link.aps.org/supplemental/10.1103/PhysRevLett.113.196802 for experimental and theoretical details as well as additional figures and discussions.
[31] P. Snijders, E. J. Moon, C. González, S. Rogge, J. Ortega, F. Flores, and H. H. Weitering, Phys. Rev. Lett. **99**, 116102 (2007).
[32] Y. Imry and M. Wortis, Phys. Rev. B **19**, 3580 (1979).
[33] C. González, F. Flores, and J. Ortega, Phys. Rev. Lett. **96**, 136101 (2006).
[34] C. González, J. Guo, J. Ortega, F. Flores, and H. H. Weitering, Phys. Rev. Lett. **102**, 115501 (2009).
[35] H. J. Kim and J. H. Cho, Phys. Rev. Lett. **110**, 116801 (2013).
[36] H. Zhang, J.-H. Choi, Y. Xu, X. Wang, X. Zhai, B. Wang, C. Zeng, J.-H. Cho, Z. Zhang, and J. G. Hou, Phys. Rev. Lett. **106**, 026801 (2011).
[37] X. H. Qiu, G. V. Nazin, and W. Ho, Phys. Rev. Lett. **93**, 196806 (2004).
[38] M. Ono, A. Kamoshida, N. Matsuura, E. Ishikawa, T. Eguchi, and Y. Hasegawa, Phys. Rev. B **67**, 201306 (2003).
[39] J. Mysliveček, A. Stróżecka, J. Steffl, P. Sobotík, I. Ošt'ádal, and B. Voigtländer, Phys. Rev. B **73**, 161302 (2006).
[40] N. Mathur and P. Littlewood, Nat. Mater. **3**, 207 (2004).